Optimization of multicore fiber for high-temperature sensing

Amy Van Newkirk,[1,*] Enrique Antonio-Lopez,[1] Guillermo Salceda-Delgado,[1,2] Rodrigo Amezcua-Correa,[1] and Axel Schülzgen[1]

[1]*CREOL, College of Optics and Photonics, University of Central Florida, Orlando, Florida 32816, USA*

[2]*CIO, Centro de Investigaciones en Optica, Leon, Guanajuato, Mexico*

**Corresponding author: amy.vannewkirk@knights.ucf.edu*

Received June 2, 2014; revised July 3, 2014; accepted July 3, 2014;
posted July 10, 2014 (Doc. ID 213110); published August 11, 2014

We demonstrate a novel high-temperature sensor using multicore fiber (MCF) spliced between two single-mode fibers. Launching light into such fiber chains creates a supermode interference pattern in the MCF that translates into a periodic modulation in the transmission spectrum. The spectrum shifts with changes in temperature and can be easily monitored in real time. This device is simple to fabricate and has been experimentally shown to operate at temperatures up to 1000°C in a very stable manner. Through simulation, we have optimized the multicore fiber design for sharp spectral features and high overall transmission in the optical communications window. Comparison between the experiment and the simulation has also allowed determination of the thermo-optic coefficient of the MCF as a function of temperature.

OCIS codes: (060.2280) Fiber design and fabrication; (060.2370) Fiber optics sensors; (280.6780) Temperature.
http://dx.doi.org/10.1364/OL.39.004812

Sensing in extreme environments, such as high temperatures, is important for various applications (e.g., downhole drilling). Generally, fiber-optic sensing requires devices with sharp spectral features that are highly sensitive to external surroundings, and can be easily interrogated within a limited spectral range. For applications requiring multiplexing, high overall transmission is also required. Fiber-optic sensing has been dominated by fiber Bragg gratings, but standard gratings suffer from degradation at temperatures above a few hundred degrees Celsius, limiting their applications. However, alternative fiber-optic devices, such as multimode interference (MMI) devices, have shown promise in sensing various environments. In the first demonstration of sensing using MMI, Layton and Bucaro showed that sound could be measured by observing the phase change between two interfering core modes in a fiber [1]. Mehta *et al.* showed a displacement sensor formed with a single-mode fiber–multimode fiber–mirror configuration [2]. Later, Li *et al.* demonstrated a temperature sensor working up to 800°C [3] using the interference of several higher order LP modes in a single-mode fiber–multimode fiber-cleaved facet configuration. However, these devices do not offer the possibility of multiplexing due to their reflective design, while transmissive elements can be multiplexed by simply splicing multiple devices together. The transmission characteristics of multimode fiber spliced between two single-mode fibers (SMS devices) have been investigated [4], and Zhang and Peng showed a transmissive refractive index sensor using an SMS structure [5].

The previously mentioned devices use either no-core or large-core step-index fiber as the fiber supporting multiple modes. However, it is also possible to sense using MMI from graded index fiber [6], photonic crystal fiber [7,8], and multicore fiber [9]. These special fiber designs lead to greater control over the modes that are interfering, and less chaotic interference patterns can be produced. Specifically, multicore fibers have shown great promise in sensing curvature [10], strain [11], and refractive index [12]. The geometry of the aforementioned multicore devices can be fairly complex, using suspended core fiber or etching of the fiber cladding. Recently, an SMS sensor utilizing photonic crystal fiber was shown to be capable of measuring 500°C [13]. This required selectively collapsing regions of the PCF, as well as precise offset splicing. A simpler fiber design will increase the applicability of the sensors, primarily when high levels of multiplexing are needed.

Demas *et al.* showed a fiber-optic sensor capable of measuring up to 1000°C with a device utilizing a PCF and a CO_2 laser-written long-period grating [14]. Unfortunately, the spectral feature they tracked was not sharp and the temperature shift was not clearly linear.

Here we show the design and optimization of a simplified SMS device utilizing multicore fiber. Recently a device has been shown to sense temperatures up to 1000°C [15]. Figure 1 is the stable response of the MCF device to temperature. This device was a 2 cm piece of seven-core fiber spliced between 2 single-mode fibers, placed in a high-temperature oven, and tracked in transmission using a broadband light source and optical spectrum analyzer.

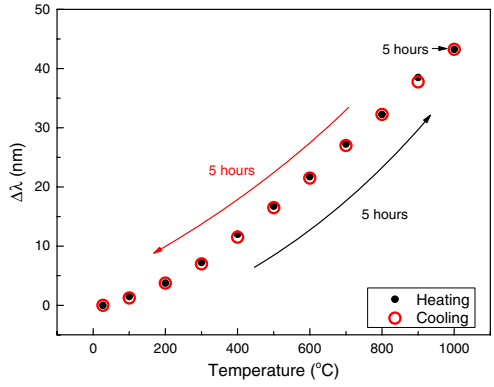

Fig. 1. Measured temperature shift of a seven-core fiber SMS device over 15 h in a high-temperature oven.

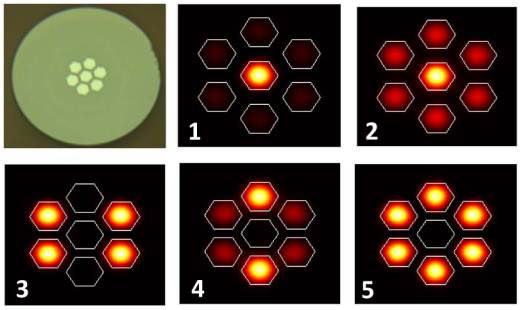

Fig. 2. Image of seven-core fiber facet and simulated supermodes supported by the seven-core fiber.

In the following, we investigate several multicore fiber designs through simulation and experiment for their use in SMS devices for highly multiplexed sensing applications. Specifically, the coupling from SMF to MCF and the supermode interference produced were studied with a focus on seven- and 19-core fiber structures, using a finite difference method (FDM) mode solver (Fimmwave, Photon Design). The FDM has previously been used for finding the modes of similar MMI fiber-sensing devices [2] A fiber with seven coupled cores supports seven supermodes, shown in Fig. 2. (Modes 3 and 4 are degenerate in intensity with differing phases across the cores.) Only two of the supermodes are excited by the fundamental mode of the SMF, modes 1 and 2, due to their circular symmetry and center-core excitation.

The interference between these two supermodes will result in a periodic coupling of the power between the center and outer cores as the light propagates down the MCF. Figure 3 shows the SMS device with supermode interference in the MCF. Spectrally, the interference generates a periodic transmission spectrum of the SMS device, shown in Fig. 5(a). The physical origin of this spectral periodicity is the difference in the propagation constants ($\Delta\beta$) of the supermodes. The wavelength dependence of $\Delta\beta$ causes the MCF to act similarly to a directional coupler, in which the coupling constant between the waveguides is directly proportional to wavelength. As the difference in propagation constants varies with wavelength, the power distribution across the cores at the facet of the second SMF will vary periodically in the spectral domain, and the amount of light collected by the second SMF will vary accordingly. The transmission modulation period and modulation depth are highly dependent on several MCF design parameters, such as number of cores, core size, and core-to-core spacing. For a seven-core fiber, the transmission spectrum is clearly periodic with sharp spectral features due to the interference of only two supermodes.

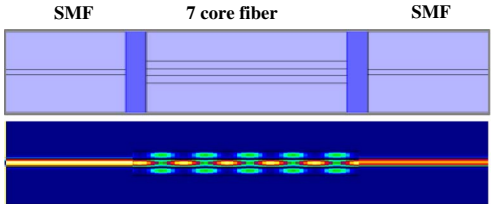

Fig. 3. Diagram of SMS device with supermode interference shown in the MCF.

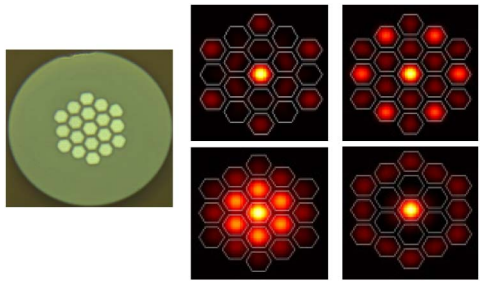

Fig. 4. Image of 19-core fiber facet and simulated supermodes excited by SMF in 19-core fiber.

In contrast, a 19-core fiber supports 19 supermodes; four are circularly symmetric modes with central-core excitation. Therefore, four supermodes are excited by the fundamental mode of SMF, as shown in Fig. 4, creating a more complicated interference pattern with more complex periodicity and less sharp spectral features.

Figure 5 shows the transmission spectra comparison between simulation and experiment for SMS devices using both seven- and 19-core fiber. The multicore fiber was fabricated from Ge-doped silica with an NA of 0.14 and group index of 1.455 and 1.454, for modes 1 and 2, respectively, at 1550 nm for the seven-core fiber. Between two sections of SMF (SMF-28 was used in all simulations and experiments), 4 cm of seven-core fiber and 12 cm of 19-core fiber were used. These lengths were chosen because of the dependence of the modulation period on the MMF length [2]. Due to the more complicated supermode interference of the 19-core fiber, the reproduction length is longer; therefore, a longer section is needed to ensure

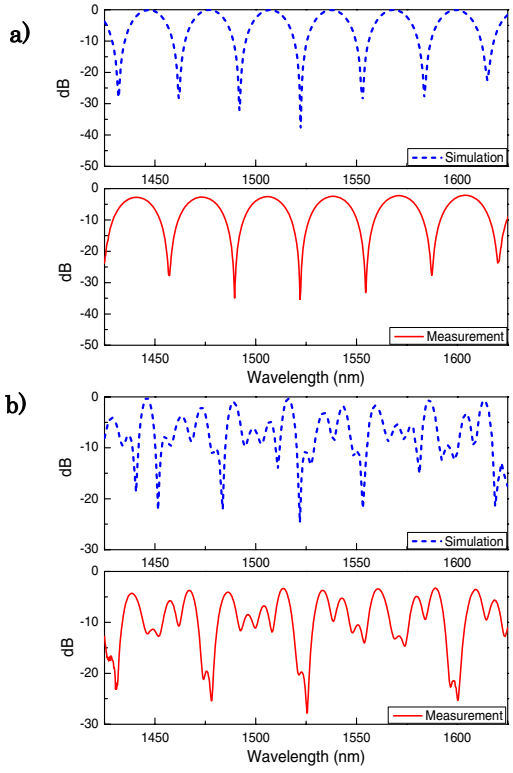

Fig. 5. Comparison of simulated and measured transmission spectra of SMS devices with 4 and 12 cm of (a) seven- and (b) 19-core fiber, respectively.

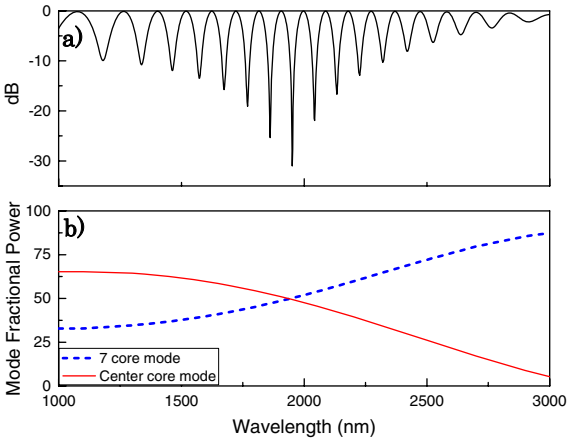

Fig. 6. SMS transmission spectrum dependence on mode fractional power in the interfering supermodes of the seven-core fiber.

several periods of modulation within the spectral range of interest. Any slight variation between the simulation and the experiment can be attributed to the margin of error in measuring the geometry and refractive index profile of the drawn fiber. Particularly, the 19-core fiber showed deformations in the outer ring of cores, shown in Fig. 4, further complicating the supermode interference and causing small differences between the experimental and simulated data.

Due to its simpler transmission spectrum with more predictability and sharper spectral features, the seven-core fiber was selected for more detailed investigation in order to obtain an optimum geometry for multiplexed temperature sensing. The requirements for multiplexing are sharp spectral features with high overall transmission between these features. Figure 6 demonstrates that maximum modulation depth occurs at equal excitation of the two interfering supermodes. This is because when the modes are equal in amplitude, complete destructive interference in the center core is possible. The fractional power excited in the supermodes depends on the mode field diameter (MFD) overlap of the fundamental mode of the SMF and the supermodes of the MCF. Due to dispersion, the MFDs are wavelength dependent. Figure 6 shows the maximum modulation depth occurring at the wavelength for which both interfering supermodes are equally excited by the SMF. With unequal mode overlap, there is still supermode interference, but the minima are less sharp. At equal coupling, the minima can reach −40 dB for the considered seven-core fiber. Therefore, when designing the SMS device, the mode coupling between the SMF and MCF must be examined for the wavelength range for which it will be interrogated in order to achieve the sharpest spectral features possible.

Two seven-core fibers were fabricated with different geometries; the difference caused by the change in MFDs of the supermodes is clearly shown when comparing the transmission spectra. The first fiber, shown in Fig. 7(a), has 9.5 μm diameter cores, a 13.6 μm pitch, and a 125 μm outer diameter. This causes unequal excitation of the two supermodes with about 61% and 38% for the center-only and all-core modes, respectively, as found through simulation. Shown in Fig. 7(c), the maximum depth of

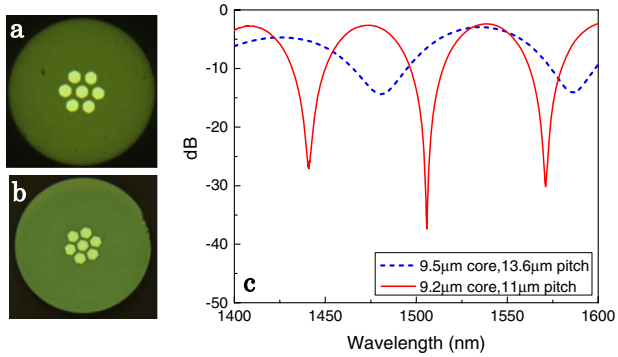

Fig. 7. Facet image of MCF with (a) 9.5 μm cores and 13.6 μm pitch, (b) 9.2 μm cores and 11 μm pitch, and (c) transmission spectra.

modulation for this fiber in an SMS device was only −12 dB.

However, the second seven-core fiber, fabricated with the same glass material and drawing parameters, has almost exactly equal mode excitation near 1550 nm. Here, the core diameter was 9.2 μm, the pitch 11 μm, and the outer diameter 125 μm. The minimum depth achieved in this case was better than −35 dB, showing the sensitivity of the SMS transmission spectrum with respect to the multicore geometry. The experiment and simulation show that the second fiber design is very close to optimal in the C-band, which is our spectral region of interest. This optimal wavelength region can be tuned over hundreds of nanometers for other applications, as needed, by changing the MCF geometry or the SMF input if the individual cores remain single mode at the selected wavelength.

Next, we focused on obtaining maximum transmission for optimal multiplexing. Maximum overall transmission occurs when the mode of the SMF can be perfectly represented by a superposition of the two excited MCF modes. Figure 8 shows that as the total excited power approaches 100% in the interfering modes, the total transmission of the SMS device also approaches 100%. High overall transmission is crucial for systems with high levels of multiplexing. Additionally, the total loss through the device, including two SMF–MCF splices, has been experimentally measured as less than 0.05 dB, showing low mode-field mismatch, low splice loss, and low propagation loss in the MCF (which is on the order of a few dB/km and, therefore, negligible for these short devices).

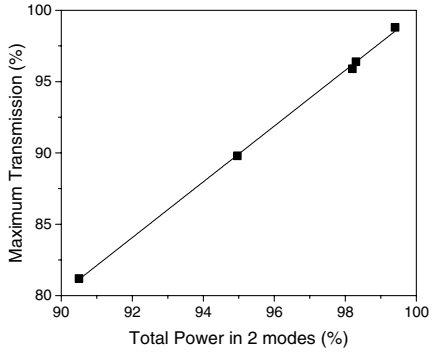

Fig. 8. Calculations showing maximum transmission occurring when power is excited in two interfering supermodes.

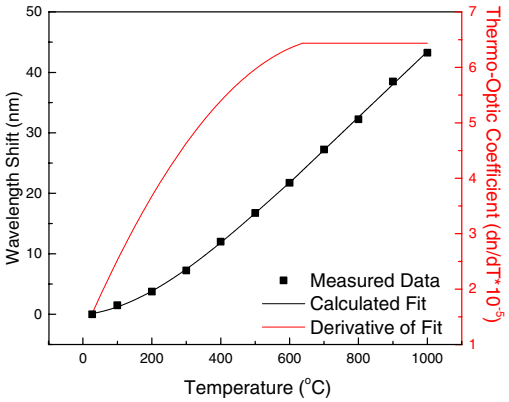

Fig. 9. Spectral shift of SMS device, with fit and calculated thermo-optic coefficient.

As this device is proposed as a temperature sensor, the sensitivity of the SMS devices to external environments has also been investigated. Using the thermal expansion and thermo-optic coefficients for silica fiber, adjustments in the refractive index and length of the MCF section can be applied, simulating temperature shifts. In simulation, the transmission spectra were shown to shift linearly with temperature for both the seven- and 19-core fibers, directly proportional to the thermo-optic coefficient (dn/dT). However, Fig. 9 shows a measurement of a seven-core SMS device, with a nonconstant slope of the wavelength shift with temperature.

A similar curve has been obtained for this temperature region by Choi *et al.* using a fiber-optic Fabry–Perot device [16]. The nonlinear wavelength shift indicates a change in the properties of the glass at different temperatures, and, therefore, a change in the thermo-optic coefficient (dn/dT). The thermal expansion coefficient of fused silica is much lower than dn/dT, and was found to be negligible for these measurements. The shift of the thermo-optic coefficient of fused silica with temperature has previously been investigated at cryogenic temperatures [17], finding a linear relationship between dn/dT and temperature. The thermo-optic coefficient in our simulation was adjusted to match the measured spectral shift, enabling the determination of dn/dT as a function of temperature for this fiber device. In Fig. 9, the wavelength shift fits a cubic function well from 0°C to 600°C, and a linear function from 600°C to 1000°C. The red curve is the derivative of the wavelength shift fitting functions, which measures the sensitivity of the SMS device as a function of temperature. Using simulation data, the sensitivity can then be correlated to the thermo-optic coefficient of the MCF. Near room temperature, the calculated thermo-optic coefficient is about 1.5×10^{-5}/°C. This value is in the range of previous measurements of fused silica at this temperature [17–19].

In conclusion, we have shown a detailed investigation of MCF-based MMI devices for use in high-temperature sensing. The supermode interference and transmission spectra of SMS devices have been simulated and matched to experimental data. Understanding the mode coupling between SMF and MCF allows for the design of devices with sharp spectral features with up to 40 dB resolution for a chosen region of the optical spectrum. We have also shown the determination of the thermo-optic coefficient of our MCF as a function of temperature. The overall high transmission enables multiplexing of a large number of devices within a narrow wavelength range for distributed sensing along a measurement chain. These sensors are simple to fabricate, requiring only two standard splices between SMF and MCF, and have been shown to operate stably in temperatures up to 1000°C. This high temperature range makes these devices suitable for industries such as down-hole drilling and in nuclear reactor facilities. Additionally, this MCF fiber is sensitive to other external changes—such as bending—increasing its range of applicability as a sensor device.

This work was supported by Faz Technology, Inc. and the Florida High Tech Corridor Council. G. Salceda-Delgado and E. Antonio-Lopez acknowledge support from CONACyT.

References

1. M. R. Layton and J. A. Bucaro, Appl. Opt. **18**, 666 (1979).
2. A. Mehta, W. Mohammed, and E. G. Johnson, IEEE Photon. Technol. Lett. **15**, 1129 (2003).
3. E. Li, X. Wang, and C. Zhang, Appl. Phys. Lett. **89**, 091119 (2006).
4. A. Kumar, R. K. Varshney, C. S. Antony, and P. Sharma, Opt. Commun. **219**, 215 (2003).
5. J. Zhang and S. Peng, in *2010 Symposium on Photonics and Optoelectronics* (IEEE, 2010), pp. 1–4.
6. S. M. Tripathi, A. Kumar, R. K. Varshney, Y. B. P. Kumar, E. Marin, and J.-P. Meunier, J. Lightwave Technol. **27**, 2348 (2009).
7. S. Silva, J. L. Santos, F. X. Malcata, J. Kobelke, K. Schuster, and O. Frazão, Opt. Lett. **36**, 852 (2011).
8. G. A. Cárdenas-Sevilla, V. Finazzi, J. Villatoro, and V. Pruneri, Opt. Express **19**, 7596 (2011).
9. A. Zhou, G. Li, Y. Zhang, Y. Wang, C. Guan, J. Yang, and L. Yuan, J. Lightwave Technol. **29**, 2985 (2011).
10. J. R. Guzman-Sepulveda and D. A. May-Arrioja, Opt. Express **21**, 11853 (2013).
11. R. M. Silva, M. S. Ferreira, J. Kobelke, K. Schuster, and O. Frazão, Opt. Lett. **36**, 3939 (2011).
12. J. R. Guzman-Sepulveda, D. Lopez-Cortes, I. Hernandez-Romano, W. Margulis, and D. A. May-Arrioja, in *Quantum Electronics, and Laser Science Conference* (Optical Society of America, 2012), paper JW2A.114.
13. F. C. Favero, R. Spittel, F. Just, J. Kobelke, M. Rothhardt, and H. Bartelt, Opt. Express **21**, 30266 (2013).
14. J. Demas, M. D. W. Grogan, T. Alkeskjold, and S. Ramachandran, Opt. Lett. **37**, 3768 (2012).
15. J. E. Antonio-Lopez, Z. S. Eznaveh, P. LiKamWa, A. Schülzgen, and R. Amezcua-Correa, Opt. Lett. **39**, 4309 (2014).
16. H. Y. Choi, K. S. Park, S. J. Park, U.-C. Paek, B. H. Lee, and E. S. Choi, Opt. Lett. **33**, 2455 (2008).
17. D. B. Leviton and B. J. Frey, "Temperature-dependent absolute refractive index measurements of synthetic fused silica," arXiv:0805.0091, (2008).
18. G. Ghosh, IEEE Photon. Technol. Lett. **6**, 431 (1994).
19. Y.-J. Kim, U.-C. Paek, and B. H. Lee, Opt. Lett. **27**, 1297 (2002).